Reflection based silicon incorporated silver coated fiber optic SPR sensor for refractive index and temperature measurement

Papiya Dhara*[1],Vinod K. Singh[2], Anupam Kumar[3], Massimo Olivero[4], Guido Perrone[4]
*[1]Department of Physics, Adamas University, Kolkata 700126, India
[2]Optical Fiber Laboratory, Department of Applied Physics, Indian Institute of Technology (Indian School of Mines) Dhanbad, 826004, Jharkhand, India
[3]Institute of Chemical Processes, Seoul National University, Seoul 08826, Republic of Korea
[4]Department of Electronics and Telecommunications (DET), Politecnico di Torino, 10129, Torino (Italy)
*Corresponding author: papiyadharaismpolito@gmail.com

Abstract

We report a reflection based multimode fiber (MMF) surface plasmon resonance (SPR) sensor utilizing a high index silicon layer between silver metal and sensing medium layer. Theoretical studies have been carried out to optimize the suitable width of material layer to sense refractive index (RI) of the analyte surrounding the optical fiber sensing region using the transfer matrix method. The RI sensitivity of the proposed SPR sensor has been experimentally verified to reach 4774 nm/RIU with figure of merit of 36.07 and resolution of 6.28×10^{-5}at 1.38 RI. Furthermore, the large thermo-optic coefficient and thermal expansion coefficient of the silicon layer has enhanced the experimental temperature sensitivity of the SPR sensor to 1.76 nm/°C.

Keywords: Surface Plasmon resonance, Fiber Optics refractive index Sensors, Temperature influence on SPR sensor, Chemical Sensing, Fiber Optics measurements

1. Introduction

Optical fiber sensing techniques have been overwhelming around the world laboratories for the last decades. The advantages of optical fiber sensors over other types of optoelectronics sensors are low fabrication cost, robustness, remote sensing and immunity to electromagnetic interface [1-6].

Among the different optical fiber sensing techniques, surface plasmon resonance (SPR) fiber optic sensors are among the most fruitful sensing techniques for real time detection and monitoring of chemical, physical and biological properties. SPR is due to the resonant, collective oscillation of electrons at the metal-dielectric (or analyte) interface stimulated by incident p-polarized light.

Previously, prism-based SPR systems have been used to generate sensing action. To achieve more convenient SPR sensors, the traditional prism-based systems have been replaced by a fiber optic design [7]. Gold is the material which has been used abundantly to produce the thin film for SPR as it has high chemical resistance. During the past few years, the real-time analysis of different biological concentration such as antibody, antigen etc. have been done successfully with SPR based gold coated optical fiber sensors [8-10]. Low cost silver metal possesses realistically good sensitivity with the sharp SPR dip. The lower d-electron energy bands than the conduction bands estimate the bulk plasma frequency in such way that the SPR probe could operate in the visible region for silver [11]. However, this plasmonic generating metal has disadvantages too as the thin layer of silver agglomerates and oxidizes in air easily [12]. Researchers have investigated earlier that a nanometer thick layer of silicon between metal and dielectric layers can increase the sensitivity of the sensor and it can protect the silver layer from oxidation too [13-16]. Recently, there are numbers of reported results in literature on optical fiber based SPR sensors for chemical and biomedical sensing application utilizing silver metal in various approaches [17-20].In this arena, the theoretical estimation has been exposed that metal coated optical fiber SPR sensors have a very weak shift in the resonance wavelength with temperature as the dielectric constant of thin metal layer, optical fiber core, and sensing layer are not strongly influenced by temperature, though temperature sensitivity may be desired in some applications [21].However, researchers have achieved enhanced sensitivity by the fiber probe coated with a silver layer into a capillary filled with thermosensitive anhydrous ethanol[22]. Liu et al. have proposed a fast response and high resolution temperature sensor designed by attaching a silicon pillar on the tip of a single-mode fiber [23].Recently, it is reported that single mode optical fibers have been coated with different metals including Sn, PbSnAg and InBito to change their sensitivity to thermal agitation and there is increasing sensitivity with temperature from 4.2 K to 50 K and decreasing sensitivity from 50 K to 60 K [24].

Wang et al. has proposed the sensitivity of the silver coated side polished fiber SPR probe up to 4365.5 nm/RIU and a FOM of 51.61 at 1.38-1.40 range [25]. In recent times, local surface plasmon resonance (LSPR) has introduced some novelty in this field by covering U shaped plastic optical fiber with silver (Ag) thin film followed by a layer of cladding synthesized by polyvinyl alcohol (PVA), graphene and silver nanoparticles. The RI sensitivity of the LSPR sensor is reported as 700.3 nm/RIU at 1.330-1.3657 RI range [26]. Zhao et al. have published the sensitivity of the SPR

based temperature sensor as 1.5745 nm/°C [22]. However, there is further scope of investigation on Ag thin film coated optical fiber-based sensor with better refractive index sensitivity and simultaneously there is requirement to produce a self-compensating RI sensor at high temperatures. Stability and repeatability are significance parameters to criticise performance of sensor and it should be investigated.

In this present study, we have experimentally studied an optical fiber SPR probe in conjunction with silicon over silver metal layer in a reflection based set up by utilizing a Y-coupler. Numerically, the thickness of silicon has been varied to optimize favourable sensitive condition of the probe and the increase in sensitivity has been obtained. Experimentally, the optical fiber SPR probe has been coated with silver mirror at the distal end of the fiber tip to increase reflectivity as well as sensitivity. The experimental RI sensitivity has been achieved about 4774 nm/ RIU with FOM 36.07 at RI 1.38 by the proposed reflection-based silver metal coated optical fiber SPR probe. The highest sensitivity has been reached by the silica incorporated SPR sensor as 1.76 nm/°C at 20°C, thus exceeding that reported in some previous researches. Repeatability and stability of the proposed sensor have been established. Decrement of temperature sensitivity at high temperature can encourage the use of the proposed RI sensor with self-compensating of temperature effects at high temperature.

The remaining of the paper is organized in four sections. Section 2 presents the theoretical background and hints about the optimization of the sensor; section 3 describes the experimental work and setup used to assess the sensor performance; section 4 reports the results along with comments and finally section 5 summarizes the results and draws the conclusions.

2. Theoretical modeling

The fabricated optical fiber SPR probe is a combination of five-layer materials as unclad multimode glass fiber core, titanium(Ti) layer, silver(Ag) layer, silicon(Si) layer and the sensing medium (analyte) respectively. The same specifications of material have been used for theoretical simulations of the SPR probe. The refractive index (RI) of the optical fiber glass core is expressed according to the Sellmeier relation [12]:

$$n(\lambda) = c_0 + c_1\lambda^2 + c_2\lambda^4 + \frac{C_3}{(\lambda^2 - l)} + \frac{C_4}{(\lambda^2 - l)^2} + \frac{C_5}{(\lambda^2 - l)^3} \quad (1)$$

where λ denotes the wavelength (in micro-meter) and the Sellmeier coefficients *l*, C_0, C_1, C_2, C_3, C_4 and C_5 have their definite numerical values. For the metal layer, we adopt noble metal (Ag) and the wavelength dependence of dielectric constant is determined from Drude model. Moreover, the RI of the analyte is limited from 1.33 to 1.38 RIU. The refractive index data of silicon at different wavelengths has been taken from reference [27].

2.1. Transfer matrix method

The useful characteristic matrix method [28, 29] can be applied to a system containing any number of layers. Also, the calculations are very easy, accurate and faithful due to absence of approximations. The multilayer model of sensor is shown in Fig.1a.

The plane-parallel layers are assumed to be stacked along the z-axis and each layer is identified by an index *k*. For the *k*-th layer, the dielectric constant, the permeability and the refractive index are denoted as ε_k, μ_k and n_k respectively. Similarly, the first and last layers are semi-infinite and the thicknesses of the other layers($d_2 \sim d_{n-1}$) are known. The tangential fields at the first boundary Z= Z_1 = 0 are related to those at the final boundary Z= Z_{n-1} by

$$\begin{bmatrix} U_1 \\ V_1 \end{bmatrix} = \underline{\underline{M}} \begin{bmatrix} U_{N-1} \\ V_{N-1} \end{bmatrix} \tag{2}$$

where, U_k and V_k, respectively, represents the tangential components of electric and magnetic fields for TE wave, and contrarily for TM wave. In addition, $\underline{\underline{M}}$ is known as the characteristic matrix of the combined structure and is given by

$$\underline{\underline{M}} = \prod_{k=2}^{N-1} \underline{\underline{M_k}} = \begin{bmatrix} M_{11} & M_{12} \\ M_{21} & M_{22} \end{bmatrix} \tag{3}$$

with

$$\underline{\underline{M_k}} = \begin{bmatrix} \cos\beta_k & -j \sin \beta_k / q_k \\ -j q_k \sin\beta_k & \cos\beta_k \end{bmatrix} \tag{4}$$

where,

$$\beta_k = \frac{2\pi}{\lambda} d_k \sqrt{{n_k}^2 - (n_1 sin\theta)^2} \quad (5)$$

and $$q_k = \sqrt{[{n_k}^2 - (n_1 sin\theta)^2]} \Big/ \mu_k \quad \text{TE wave} \quad (6a)$$

$$q_k = \sqrt{[{n_k}^2 - (n_1 sin\theta)^2]} \Big/ \epsilon_k \quad \text{TM wave} \quad (6b)$$

The amplitude reflection coefficient is given by

$$r = \frac{(M_{11}+M_{12}q_N)q_1-(M_{21}+M_{22}q_N)}{(M_{11}+M_{12}q_N)q_1+(M_{21}+M_{22}q_N)} \quad (7)$$

Finally, the power reflectivity for the p-polarized light is

$$R = | r^2 | \quad (8)$$

It is considered in experimental and theoretical analysis that all guided rays are launched inside the optical fiber which is the cylindrical geometry though the numerical analysis is based on planar geometry. It has been also reported earlier that both the meridional and skew rays are propagated through the cylindrical geometry and the skew rays decreases the sensitivity of the sensor [30]. In our present study, the propagation of skew rays has been avoided intentionally for the sake of simple simulation.

The normalized transmitted power collected at the end of the optical fiber can be expressed as:

$$P_{trans} = \frac{\int_0^{\alpha max} \int_{\theta_{cr}}^{\pi/2} {R_p}^{N_{ref}(\theta,\alpha)} \frac{n^2 sin\theta cos\theta}{(1-n^2 cos^2\theta)^2} \cos\theta_s d\theta d\alpha}{\int_0^{\alpha max} \int_{\theta_{cr}}^{\pi/2} \frac{n^2 sin\theta cos\theta}{(1-n^2 cos^2\theta)^2} \cos\theta_s d\theta d\alpha} \quad (9)$$

where,

$$N_{ref}(\theta, \alpha) = \frac{L}{Dtan\theta} \quad (10)$$

$$\theta_{cr} = \sin^{-1}\frac{n_{cl}}{n^{i}} \quad (11)$$

$N_{ref}(\theta, \alpha)$ represents the total number of reflections performed by a ray of angle θ with the normal to the core-metal layer interface and skewness angle α in the sensing region. *L* and *D* represent the length of the sensing region and the fiber core diameter respectively. θ_{cr} is the critical angle of the fiber, and n_{cl} is the refractive index of the cladding of the fiber.

Numerically, the thicknesses of the titanium and silver have been optimized as 5 nm and 50 nm respectively. The Silicon layer width has been varied as 5 nm, 7 nm and 10 nm respectively to attain enhancement in sensitivity. Finally, the thickness of Si layer has been found as10 nm appealing highest sensitivity for the proposed model.

3. Fiber probe fabrication & experiment

3.1. Method of probe fabrication

The fiber chosen to carry out the experiment is MMF with silica core diameter of 600±10 μm for suitable handling. The used MMF with Tetraethyl orthosilicate polymer cladding (Thorlabs, FT600UMT) has perfect specifications to validate SPR experiment.

The cladding has been removed by acetone from a 2 cm-long section. Then, the unclad portion of the fiber has been coated with 5 nm titanium and 50 nm silver in vacuum at 5×10^{-5} Pa pressure by thermal evaporation technique. The thickness of the silver layer, which is a typical value used in both prism- and fiber- SPR sensors, is optimized for the highest SPR response, according to previous simulations and investigations [31,32]. The thin layer of titanium is deposited in order to enhance the adhesion of silver to the glass, while yielding negligible perturbation on the SPR response. The additional layer of silicon of thickness 10 nm has been deposited over silver using the same technique. The thickness of the deposited layers is very well controlled by the sputtering/evaporation process. The deposition time has been previously calibrated so that layers can be deposited with a sub-nm accuracy. The thickness of different materials has been estimated during theoretical modelling of the material layers using MATLAB.

The cross-section of the one end of the silver coated fiber has been dipped within Tollen's reagent and a very thin silver mirror has been formed at the distal end of the silver coated fiber (Fig.1b & d). In this case the thickness of the silver layer is controlled by the dipping time, but it is not a critical parameter, since its purpose is to make the sensor working in reflection and as long as the reflected signal is sufficient to be readable by the interrogation system, there is no constraint on this deposition. However, it has been verified that the reflectance of the SPR probe reaches 90% in a typical fabrication process.

3.2. Experimental procedure

The reflection based set up has been arranged as shown in Fig. 1c.The broad band LED source (470 nm to 850 nm) is attached with one arm of Y-type fiber optic coupler (BIF600-VIS-NIR, Ocean Optic Corporation) and other arm of coupler is connected to a spectrometer (Ocean Optics USB2000+) as detector. The coupler has been utilized to launch the light through coated SPR fiber probe and receive the SPR spectrum of the transmitted light after reflection by the silver mirror at the distal end of the probe. The described SPR probes have been positioned in vertical displacement stand and immersed within experimental solutions to detect SPR curves. To get an accurate evaluation of the SPR wavelength, output SPR curves have been fitted using a Lorentzian function.

The set of solutions having different refractive indices (1.33-1.38) have been prepared with proper mixing of sugar-water in weight/volume% concentration and pure water for RI sensing. The refractive indices of these solutions have been measured by Abbe refractometer. To compensate the error from the measurement process, three cycle of the same experiment have been carried out. The temperature sensing experiment has been carried out by immersing the Ag-Si coated fiber probe in heated sodium chloride solution having RI 1.367. Afterwards, the transmittance SPR spectra have been detected during mild temperature fall period of sodium chloride solution from 95° to 20°C.The environmental temperature has been kept constant throughout the experiment.

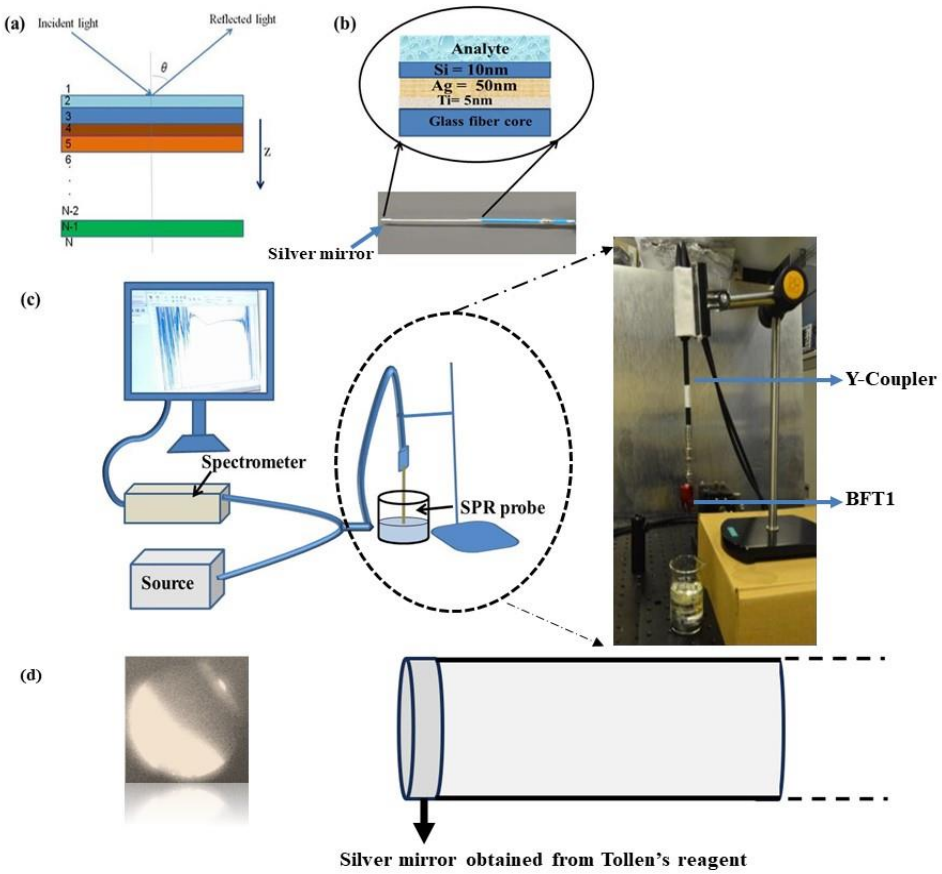

Fig.1. (a) The multilayer model of sensor in transfer matrix method (b) 5nm Ti, 50nm Ag and 10nm Si coated optical fiber SPR probe (Inset: Real image of coated optical fiber with silver mirror at end) (c) The reflectance based set up of SPR (Inset: Real image of Y-coupler connected with optical fiber probe through bare optical fiber terminator; BFT1, Thorlabs) (d) Cross-section view of silver mirror coated optical fiber termination (left) and correspondent side-view schematic of the tip (right).

4. Results and discussion

4.1. Numerically calculated SPR probe sensitivity

Transfer matrix method has been utilized to determine power reflectivity of the p-polarized light launched within fiber core and ultimately the SPR curves are obtained by MATLAB simulation.The SPR wavelength has been estimated at the minimum dip of the transmittance power of the SPR curves. Fig 2a represents the SPR wavelength shift with RI of analyte surrounding the coated region from 1.33 to 1.38. The impact of the 5 nm silicon layer combined with 5 nm titanium and 50 nm silver combinationis shown in this plotting as a sharper SPR wavelength shift with RI.

Fig. 2b shows the increasing sensitivity of this combination with the increasing silicon width which is reached upto 5700 nm/RIU for 10 nm silicon width at 1.38 with FOM 169.32 and resolution 5.260×10^{-5}.

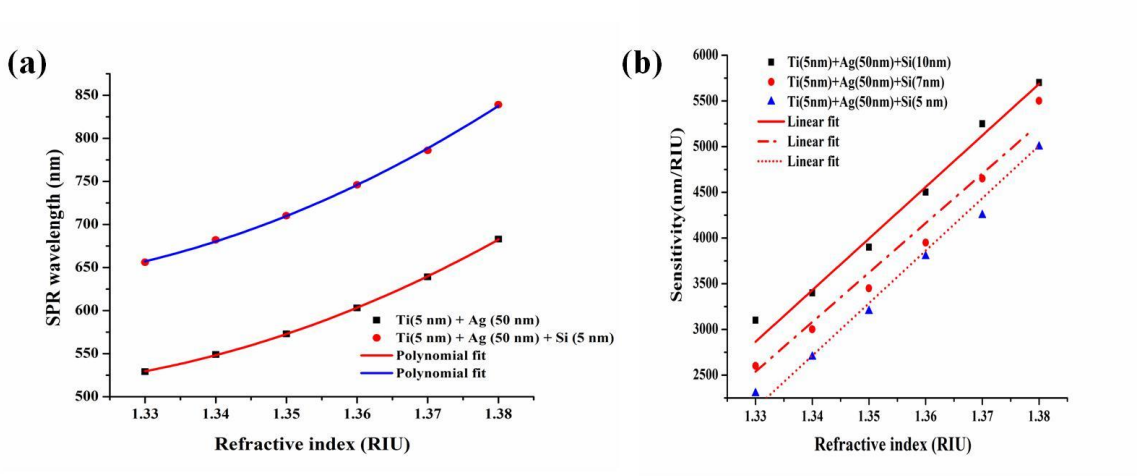

Fig.2. Theoretically simulated graphs (a) for SPR wavelength variation with RI (b) for sensitivity variation with RI.

4.2. Normalized Transmittance spectra and SPR wavelength shift with RI

The experimental normalized transmittance spectra obtained by the fabricated SPR probe is shown in inset of the Fig. 3. It is depicted by the spectra that there is the SPR dip shift with variation of RI and the SPR dips are distinguishable to each other. Therefore, the SPR wavelength can be determine by Lorentz fitting of the SPR curves. It shows that there is sharp shift of SPR dip towards longer wavelength with increasing RI of analyte surrounding sensing surface. Furthermore, it can be noted that the SPR curves broaden gradually with increasing RI of analyte. The variation of SPR wavelength with RI has been plotted in Fig. 3. It is observed that the SPR wavelength increases with increase of RI.

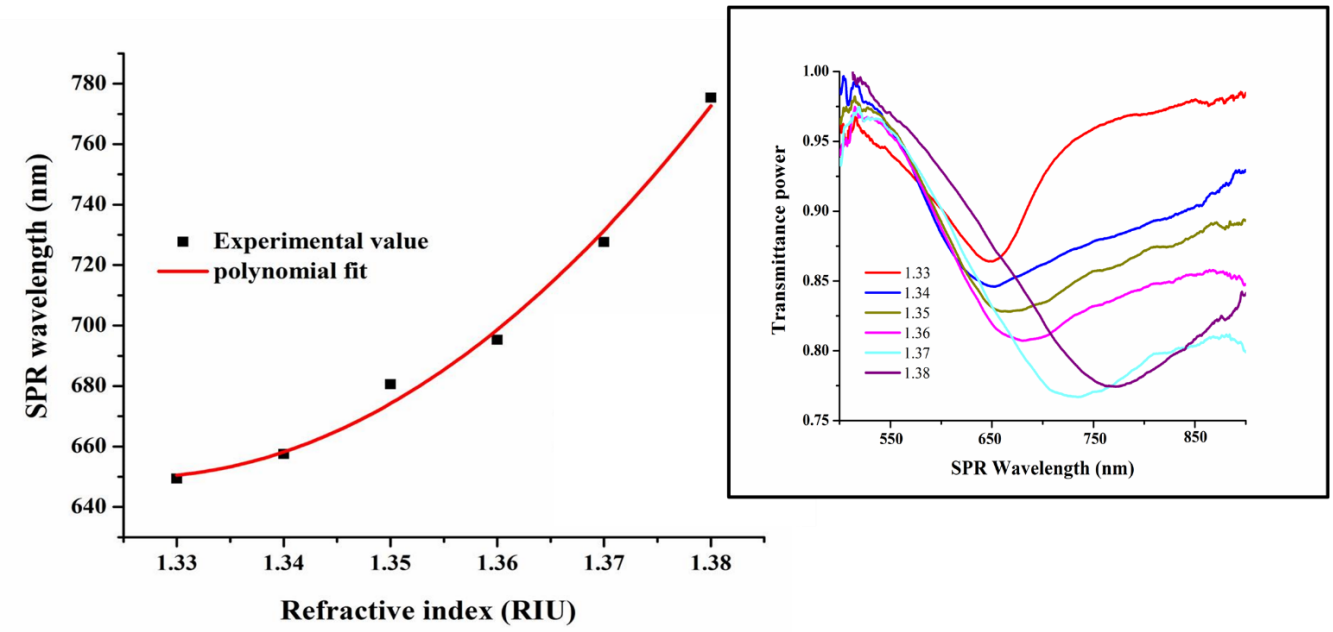

Fig.3. Experimental SPR wavelength shift with RI by 5nm Ti, 50nm Ag and 10nm Si coated probe & experimental transmittance SPR spectra (inset).

4.3. Sensitivity, figure of merit (FOM) & resolution for RI sensor

Sensitivity, figure of merit and resolution performance parameters of the SPR based RI sensor are determined from the simulated and experimental results. Sensitivity is calculated as the slope of the calibration curve at a given refractive index. The width of the SPR curve has major role in the accuracy determination of the resonance wavelength. To get the overall performance of the sensor, the figure of merit (FOM) is defined as the ratio of the sensitivity and the full width at half maxima (FWHM) [33]. The resolution of the SPR-based optical RI sensor is the minimum amount of change in refractive index detectable by the sensor.

From Fig.3, it is possible to determine slope of the calibration curve at each RI point which calculate sensitivity of the probe at the corresponding RI point. Theoretical and experimental study represents the sensitivity of the probe as a function of RI as shown in Fig.4. Furthermore, it is depicted as linear relationship. The calculated FOM increases from 2.70-36.07 with increase of RI.

There is discrepancy between the theoretical and experimental value of these performance parameters. It is because of an approximation taken in theoretical study that skew ray is not present in guided ray. In practice, the combinations of skew and meridional rays propagate within fiber

core and skews ray decreases sensitivity. The calculated performance parameters of the present SPR probe are mentioned in Table 1.

To compare the values of performance parameter obtained in the present experimental study with previous research, we have tabulated the values of the sensitivity of the various proposed Ag coated fiber optic SPR RI sensor in Table 2.

It can be noted that the RI sensitivity obtained in the present study is higher than most of those reported in the recent literature. There are experimental investigations that claim higher sensitivities, such as [34], but this is based on the use of hollow core fiber, or rather a silica capillary, which is not an off-the-shelf product and it may be difficult to handle (splicing to standard fibers for interfacing to instruments can be very critical), whereas the research here presented exploits a cost-effective commercial fiber and low-cost easy-to implement sensor fabrication procedures and it works as an all-fiber sensor with no butt-couplings or mechanically unstable connections; furthermore, in contrast to ref [34] in works in reflection and therefore can be easily used as a probe. Here the nanometres-thick high refractive index silicon layer, which enhances the field intensity at the silicon analyte interface, is responsible for the improved sensitivity and it comes at no additional cost since it only involves an extra layer deposition. Furthermore, the thin titanium layer that increases the adhesiveness of the plasmonic metal on glass surface may also represent an extra source of the enhanced RI sensitivity.

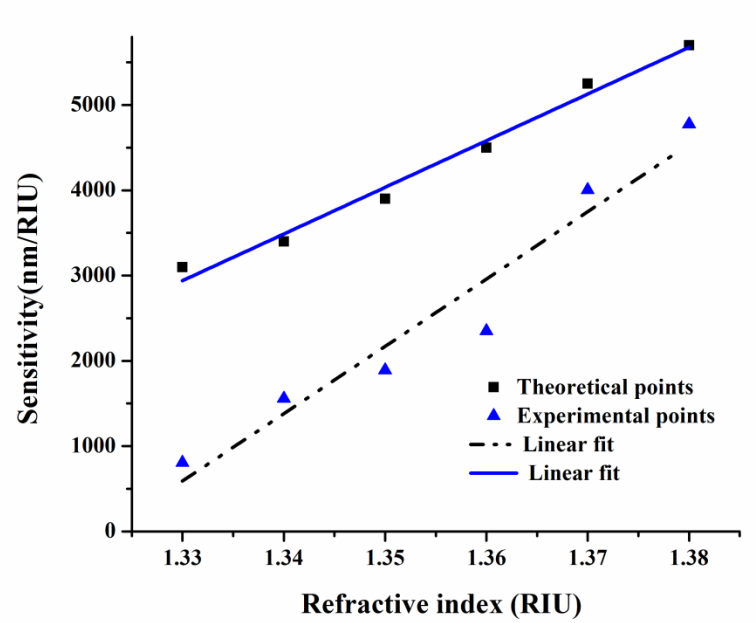

Fig.4. Theoretical and experimental comparison of RI sensitivity of 5nm Ti, 50nm Ag and 10nm Si coated SPR probe.

Table 1: Theoretical and experimental performance parameters of RI sensor.

Structure details	Sensitivities (nm/RIU) in 1.33-1.38 RI range	Resolution in 1.33 – 1.38 RI range
Glass fiber core , 5nm Ti, 50nm Ag, analyte (Simulated)	2000 – 4400	1.5×10^{-4} -6.81×10^{-5}
Glass fiber core, 5nmTi, 50nm Ag, 5nm Si,analyte (Simulated)	2300 - 5000	1.30×10^{-4} – 6×10^{-5}
Glass fiber core, 5nmTi, 50nm Ag, 7nm Si,analyte (Simulated)	2600-5500	1.51×10^{-4}- 5.45×10^{-5}
Glass fiber core, 5nmTi, 50nm Ag, 10nm Si,analyte (Simulated)	3100-5700	9.67×10^{-5}- 5.26×10^{-5}
Glass fiber core, 5nmTi, 50nm Ag, 10nm Si,analyte(Experimental)	808-4774	3.71×10^{-4}- 6.28×10^{-5}

Table 2: Comparison of present data with previously published work of SPR RI sensor.

Characteristics of the sensor	Detection RI	Sensitivity(nm/RIU)	Reference
Unclad MMF, Ag–Au thin film	1.40	590	[35]

Unclad MMF, Au–Ag alloy nanoparticle	1.34	3000	[36]
Unclad MMF, Ag end mirror, Ag coating, SiO layer	1.41	3800	[37]
SMF, side polished, Ag coating	1.40	4365.5	[25]
Unclad MMF,Ag end mirror, Au-Ag alloy nanoparticle	1.30-1.40	650	[18]
MMF, Ag nanoparticle fiber end	1-1.5	67.6	[17]
U shaped plastic optical fiber, Ag thin film, PVA, graphene and silver nanoparticles	1.33-1.36	700.3	[26]
LSPR GK570/Ag coated hollow fiber	1.47 to 1.51	12500	[34]
Present study	1.38	4774	

294
295
296
297 *4.4. Stability and repeatability of RI sensor*
298
299 Stability and repeatability of the described RI sensors have been examined for possible application
300 in a real framework. The transmittance SPR spectra have been collected for 17 hours after
301 immersing the proposed SPR probe in water. Thereafter, by analysing the SPR dip for each graph
302 collected, the variation of the SPR dip wavelength with time is plotted in Fig. 5, showing a
303 maximum 0.5 nm wavelength shift. The small variation of the SPR wavelength is ascribed to
304 environmental variations (e.g., temperature) and it is believed to be monotone just by coincidence.
305 However, the long-time monitoring demonstrates a consistent stability of this RI sensor.
306 The RI sensitivities of the described sensor probe have been calculated at 1.33-1.38 range in 15
307 days interval experiment. Fig. 6 describes the worthy repeatability of the RI sensitivity of the
308 proposed sensor.
309
310

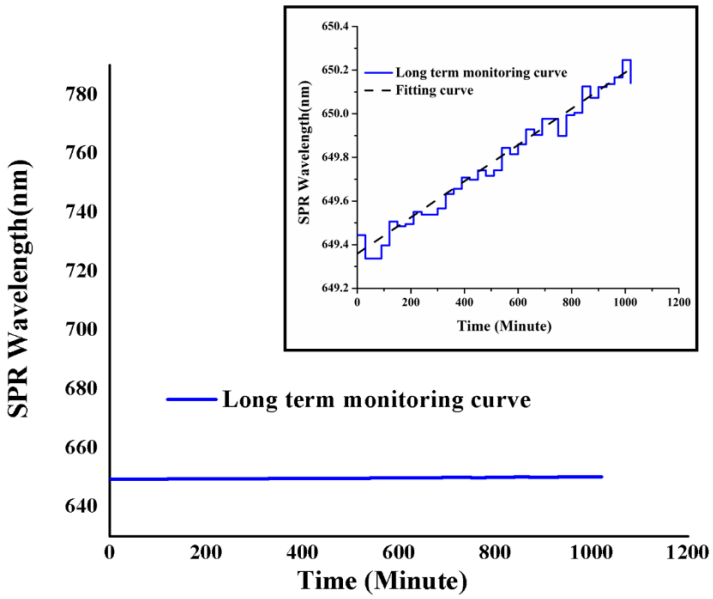

Fig.5.The SPR wavelength versus time at 1.33 RI for 17 hours monitoring (Inset: Comprehensive view of wavelength shift with time).

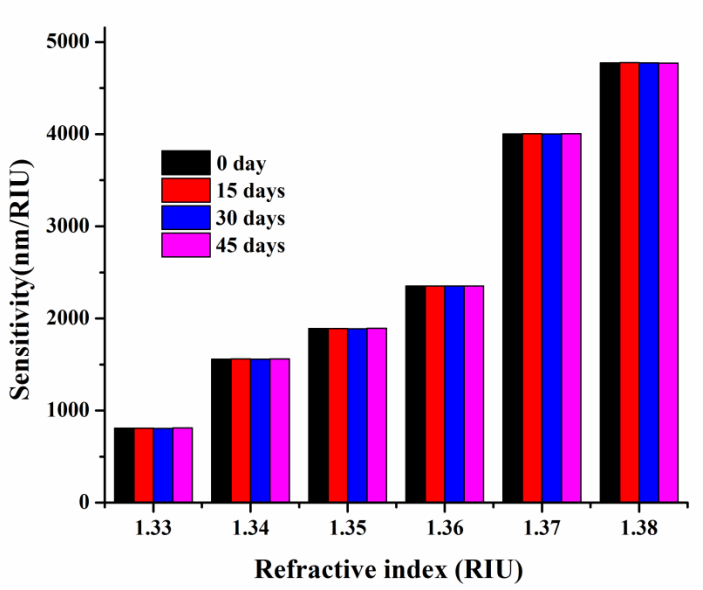

Fig.6.The experimental RI sensitivity from 1.33-1.38 RI in 15 days interval.

4.5. Heating effect on the SPR probe

In addition to the application of the sensor, temperature sensitivity is another advantage of the proposed silicon incorporated SPR probe due to high thermo-optic coefficient and thermo-expansion coefficient of silicon. It is observed from experimental SPR spectra (Fig. 7 inset) that there is a noticeable red shift of SPR wavelength with the decreasing temperature of the sodium chloride solution having RI 1.367 from 95°C to 20°C. The slope of the calibration curve at each temperature point is the temperature sensitivity of the SPR sensor at that particular temperature and these are calculated as 0.48 nm /°C, 0.56 nm /°C, 1.20 nm /°C and 1.76 nm /°C at 95°C, 70°C , 45 °C and 20°C respectively. Theoretically it has been reported that the temperature sensitivity of SPR based sensor is inversely proportional to the increasing temperature [21]. Therefore, on the basis of this statement, the temperature response of the present SPR sensor is justified. Table 3 illustrates a comparison of the present obtained temperature sensitivity with some latest published results by focussing on Ag coated optical fiber SPR based temperature sensors.

This comparison shows that the presented sensor has a similar temperature response to that of [22] and one order of magnitude higher than that based on silver-coated fiber Bragg grating [28]. Whereas at ambient temperature the presented sensor could be used as an effective temperature transducer, its decreasing sensitivity at high temperatures may be exploited for self-compensation of temperature effects during RI measurements. However, this possibility, along with a deeper investigation on the physical effect of the silicon layer on the temperature sensitivity shall be further carried out through simulation and experiments.

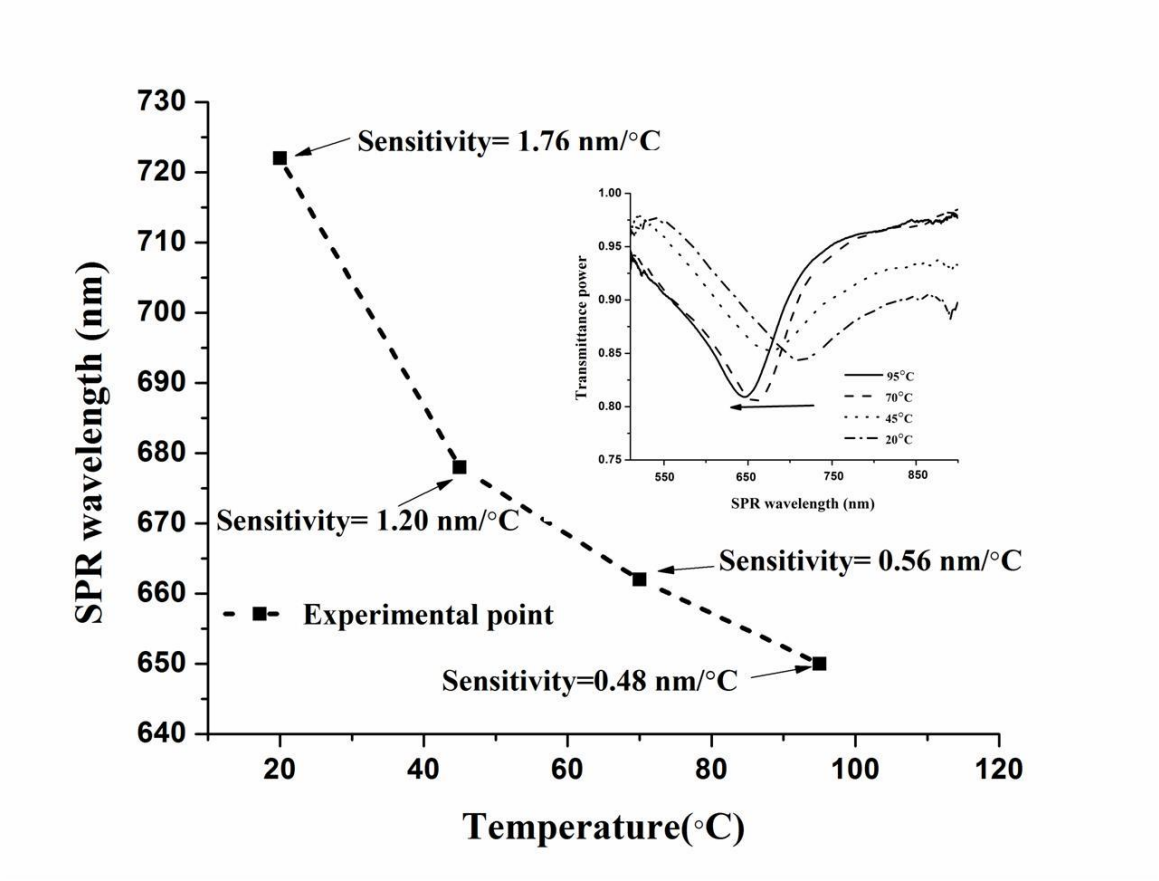

Fig.7: The SPR wavelength variation with temperature and the corresponding SPR transmittance spectra (inset) for 30% sugar-water solution concentration .

Table 3: Comparison of present data with previously published literature about SPR temperature sensors.

Characteristics of the sensor	Sensitivity(nm/°C)	Reference
Unclad MMF, Ag coating, covered by capillary filled with ethanol	1.574	[22]
MMF-FBG-MMF, Ag coating on outer face of cladding of FBG	0.172	[38]
Present study	1.760	

5. Conclusions

A reflection-based silver-silicon coated over unclad core of multimode fiber SPR probe has been proposed and characterized successfully. Theoretically, the width of coated materials is optimized to Ti (5nm), Ag (50nm) and Si (10nm) and modeling results a high RI sensitivity of 5700 nm/RIU

with FOM 169.32 and resolution 5.260× 10^{-5} at 1.38 RI. An effort has been made to build a reflection based experimental SPR set up by using MMF with coated layer of Ti-Ag-Si of optimized specifications with Y-coupler and mirror at distal end of the fiber. It is significant that with the increase of RI, sensitivity and FOM have been increased and the resolution has been decreased. The sensitivity has been found higher than reported in literature as 4774 nm/RIU with FOM 36.07 and resolution 6.284×10^{-5} at 1.38 RI. Utilizing the high thermo-optic coefficient and thermo-expansion coefficient of silicon layer, the proposed SPR sensor has been established as temperature sensor of 1.76 nm /°C sensitivity at 20°C. Proposed sensor has been monitored for 17 hours duration and negligible wavelength shift is found at constant RI. RI sensitivity of the described sensor remains unchanged at 1.33-1.38 RI range in 15 days interval experiment. Thus, Stability and repeatability of the proposed sensor have been established. Significantly, the proposed sensor shows decrease of temperature sensitivity at high temperature and it could represent the RI sensor with self-compensating of temperature effects. The proposed SPR sensor could be low cost, stable and re-usable in numerous fields.

References

[1] Alan D. Kersey, A Review of Recent Developments in Fiber Optic Sensor Technology, Opt. Fiber Technol. 2(1996) 291–317.

[2] Byeong Ha Lee, Young Ho Kim , Kwan Seob Park , Joo Beom Eom , Myoung Jin Kim, Byung Sup Rho, Interferometric Fiber Optic Sensors, Sensors 12(2012) 2467-2486.

[3] P. Dhara, Vinod K. Singh, Effect of MMF stub on the sensitivity of a photonic crystal fiber interferometer sensor at 1550 nm Opt. Fiber Technol. 21(2015) 154–159.

[4] P. Dhara, Vinod K. Singh, Improved mesostructure by incorporating surfactant on thin film to avail advance optical fiber pH sensor with temperature cross sensitivity feature, Laser Phys. 27(2017)035101.

[5] Rahul Kumar Gangwar, Vinod Kumar Singh, Highly Sensitive Surface Plasmon Resonance Based D-Shaped Photonic Crystal Fiber Refractive Index Sensor, Plasmonics 12(2017) 1367–1372.

[6] Yu Qian, Yong Zhao, Qi-lu Wu, Yang Yang, Review of Salinity Measurement Technology Based on Optical Fiber Sensor, Sens. Actuators, B 260(2018)86-105.

[7] R.C. Jorgenson, S.S.Yee, A fiber-optic chemical sensor based on surface plasmon resonance, Sens. Actuators, B 12(1993) 213–220.

[8] Yuhki Yanase, Takaaki Hiragun, Kaori Ishii, Tomoko Kawaguchi, Tetsuji Yanase, Mikio Kawai, Kenji Sakamoto, Michihiro Hide, Surface Plasmon Resonance for Cell-Based Clinical Diagnosis, Sensors 14(2014) 4948-4959.

[9] Wenjia Wang, Zhigang Mai, Yuzhi Chen, Jiaqi Wang, Liang Li, Qingning Su, Xuejin Li, Xueming Hong, A label-free fiber optic SPR biosensor for specific detection of C-reactive protein, Sci. Rep.7(2017)16904.

[10] Wei Peng, Soame Banerji, Yoon-Chang Kim, Karl S. Booksh, Investigation of dual-channel fiber-optic surface plasmon resonance sensing for biological applications, Opt. Lett. 30 (2005) 2988–2990.

[11] Crissy Rhodes, Stefan Franzen, Surface plasmon resonance in conducting metal oxides, J. Appl. Phys. 100(2006) 054905.

[12] A.K.Sharma, Banshi D. Gupta, On the sensitivity and signal to noise ratio of a step-index fiber optic surface plasmon resonance sensor with bimetallic layers, Opt. Commun. 245(2005) 159–169.

[13] Amit Lahav, Mark Auslender, I. Abdulhalim , Sensitivity enhancement of guided-wave surface-plasmon resonance sensors, Opt. Lett. 33 (2008) 2539-2541.

[14] A.Shalabney, I. Abdulhalim, Figure-of-merit enhancement of surface plasmon resonance sensors in the spectral interrogation, Opt. Lett. 37(2012) 1175-1177.

[15] Priya Bhatia, Banshi D. Gupta, Fabrication and characterization of a surface plasmon resonance based fiber optic urea sensor for biomedical applications, Sens. Actuators, B 161(2012) 434-438.

[16] Priya Bhatia, Banshi D.Gupta, Surface-plasmon-resonance-based fiber-optic refractive index sensor: sensitivity enhancement, Appl. Opt. 50 (2011) 2032-2036.

[17] J. Gabriel Ortega-Mendoza, Alfonso Padilla-Vivanco, Carina Toxqui-Quitl, Placido Zaca-Morán, David Villegas-Hernández, Fernando Chávez , Optical Fiber Sensor Based on Localized Surface Plasmon Resonance Using Silver Nanoparticles Photodeposited on the Optical Fiber End, Sensors14(2014)18701-18710.

[18] Hieu Tu, Tong Sun, Kenneth T. Grattan, SPR-based optical fber sensors using gold-silver alloy particles as the active sensing material, IEEE sens. J 13(2013) 2192-2199.

[19] Ahmmed A Rifat, G Amouzad Mahdiraji, Desmond M Chow, Yu Gang Shee, Rajib Ahmed, Faisal Rafiq Mahamd Adikan, Photonic Crystal Fiber-Based Surface Plasmon Resonance Sensor with Selective Analyte Channels and Graphene-Silver Deposited Core, Sensors15(2015) 11499-11510.

[20] Tuan Guo, Fu Liu, Xing Liang, Xuhui Qiu, Yunyun Huang, Chen Xie, Peng Xu, Wei Mao, Bai-Ou Guan, Jacques Albert, Highly sensitive detection of urinary protein variations using tilted fiber grating sensors with plasmonic nanocoatings Biosensors and Bioelectronics 78(2016) 221–228.

[21] Anuj K. Sharma, Banshi D. Gupta, Influence of temperature on the sensitivity and signal-to-noise ratio of a fiber-optic surface plasmon resonance sensor, Appl. Opt.45 (2006)151-161.

[22] Yong Zhao, Ze-Qun Deng, Hai-Feng, Fiber-Optic SPR Sensor for Temperature Measurement, IEEE Trans Instrum. Meas.64 (2015) 3099 – 3104.

[23] Guigen Liu, Ming Han, Weilin Hou, High-resolution and fast-response fiber-optic temperature sensor using silicon Fabry-Pérot cavity, Opt. Express 23(2015) 7237-7247.

[24] Federico Scurti, John Mcgarrahan, Justin Schwartz, Effects of metallic coatings on the thermal sensitivity of optical fiber sensors at cryogenic temperatures, Opt. Mater. Express 7(2017) 1754-1766.

[25] Jing Zhao, Shaoqing Cao, Changrui Liao, Ying Wang, Guanjun Wang, Xizhen Xu,Cailing Fu, Guiwen Xu, Jiarong Lian, Yiping Wang, Surface plasmon resonance refractive sensor based on silver-coated side-polished fiber, Sens. Actuators, B 230(2016) 206-211.

[26] Shouzhen Jiang, Zhe Li, Chao Zhang, Saisai Gao, Zhen Li, Hengwei Qiu, Chonghui Li, Cheng Yang, Mei Liu, Yanjun Liu, A novel U-bent plastic optical fibre local surface plasmon resonance sensor based on graphene and silver nanoparticles hybrid structure, J. Phys. D: Appl. Phys. 50(2017)165105.

[27] SOPRA N&K Database, www.refractiveindex.info.

[28] Max Born, Emil Wolf, Principles of optics, Cambridge University Press (2002) Cambridge, UK, 7thed.

[29] RanaTabassum, Banshi D. Gupta, SPR based fiber-optic sensor with enhanced electric field intensity and figure of merit using different single and bimetallic configurations, Opt. Commun. 367(2016) 23–34.

[30] Yogendra S. Dwivedi, Anuj K. Sharma, Banshi D. Gupta, Influence of skew rays on the sensitivity and signal-to-noise ratio of a fiber-optic surface-plasmon-resonance sensor: a theoretical study, Appl. Opt. 46(2007) 4563–4569.

[31] Papiya Dhara, Vinod Kumar Singh, Massimo Olivero, Guido Perrone, Reflectance-based low-cost disposable optical fiber surface plasmon resonance probe with enhanced biochemical sensitivity, Optical Engineering (2016), 55, p. 46114.

[32] Hitoshi Suzuki, Mitsunori Sugimoto, Yoshikazu Matsui, Jun Kondoh, Effects of gold film thickness on spectrum profile and sensitivity of a multimode-optical- fiber SPR sensor, Sensors and Actuators B: Chemical (2008), 132, pp. 26-33.

[33] A.Shalabney, I.Abdulhalim, Figure-of-merit enhancement of surface plasmon resonance sensors in the spectral interrogation, Opt. Lett. 37(2012) 1175–1177.

[34] Zhao, Xiao, Xian Zhang, Xiao-Song Zhu, and Yi-Wei Shi. "Long range surface plasmon resonance sensor based on the GK570/Ag coated hollow fiber with an asymmetric layer structure." Optics express 27, no. 7 (2019): 9550-9560.

[35] M.Kanso, S.Cuenot, G.Louarn, Sensitivity of Optical Fiber Sensor Based on Surface Plasmon Resonance: Modeling and Experiments, Plasmonics 3(2008) 49–57.

[36] Anuj K Sharma, B D Gupta, Fibre-optic sensor based on surface plasmon resonance with Ag–Au alloy nanoparticle films, Nanotechnol. 17(2006) 124–131.

[37] Jie Zeng, Dakai Liang, Application of fiber optic surface plasmon resonance sensor for measuring liquid refractive index, J. Intell. Mater. Syst. Struct. 17(2006) 787–791.

[38] Tao Hu, Yong Zhao, An-ning Song, Fiber optic SPR sensor for refractive index and temperature measurement based on MMF-FBG-MMF structure, Sens. Actuators, B 237 (2016) 521–525.